Chapter 2

Mechanical Behavior Analysis and Testing of Marine Riser in Deepwater Drilling

Yanbin Wang, Deli Gao and Jun Fang

Additional information is available at the end of the chapter

http://dx.doi.org/10.5772/62315

Abstract

In this chapter, the mechanical model and control equation have been established to analyse the mechanical behaviour of marine riser in working condition. The control equation has been solved by weighted residual method, and the analysis model has been verified by finite element method (FEM) in ABAQUS framework. Based on this, the deformation and stress distribution of the marine riser have been acquired. Then, a simulation experimental system has been introduced, and the system composition, functions and operational approach of the experimental setup have been stated in detail. After that, a tubular sample has been manufactured to simulate the marine riser, and the simulation experiments have been carried out based on this setup, where the experimental procedures, key aspects, difficult points of the experiment and its corresponding solutions have been elaborated. At last, the strain value of the specimen has been measured successfully after the experiment, and the stress state of the specimen has been obtained based on the analysis.

Keywords: Deepwater drilling, Marine riser, mechanical behaviour, Simulation experiment, Stress state testing

1. Introduction

The exploration and development of offshore oil and gas resources are gradually from shallow to deep sea area. The special sea state conditions and engineering problems in deepwater put forward higher request to the drilling technology, and a higher level of drilling equipment and techniques are urgently need to face the challenges.

Generally, the technical challenges in deep offshore drilling include: (1) water depth—huge drilling platform or drilling ship is needed in deepwater drilling. Moreover, the underwater equipment and tools must be precision, intelligent and flexible with higher reliability. The gravity of drilling riser and the complexity of marine environment increase with water depth. Therefore, the drilling vessel must have sufficient bearing capacity and deck space. (2) Sea wave and current—deviation of drilling vessel will occur under the action of sea wave and current, which will result in riser deformation and stress re-distribution. Riser under dynamic lateral force deduced by sea wave and current will generate vortex-induced vibration (VIV), which puts forward higher requirements on fatigue strength design of offshore pipelines. What's more, during drilling operation, riser is needed to disconnect from subsea wellhead and suspended on the drilling vessel, which will cause dynamic compression and even local instability. (3) Narrow drilling mud density window—the undercompaction of deepwater formation causes narrow drilling mud density window, which will result in frequent drilling accidents, such as lost circulation, well kick, borehole collapse and sticking. Besides, the narrow window will bring about the increase of casing layers even unable to drill to the target stratum. Meanwhile, well control problems always exist in narrow window condition [1]. (4) Geological disasters—geological disasters in deepwater drilling mainly include loose submarine soil and shallow flow. Sinking of subsea wellhead, blowout preventer (BOP) and surface conductor will appear if shallow flow is serious. When gas in shallow flow enters the sea water, the density of sea water and the buoyancy of drilling vessel will decrease, which will cause big accident and even rig capsized. (5) Well control—the well-control risk of drilling equipment, submarine tools and hydrate problems is also remarkable [2].

Various tubulars, such as drilling riser, drilling pipe, production tubulars and subsea tubulars, are indispensable for deepwater exploration and development. These pipelines are subjected to kinds of loads under service condition, and how to ensure the security of them is the foundation of efficiently acquiring oil and gas in deepwater. Taking the drilling riser as example, the operating loads subjecting to the riser include internal pressure, external pressure, axial tension, lateral force generated by sea wave and current and top displacement resulted from floating vessel, which can cause kinds of failure models, such as wear, rupture and collapse. Besides theory analysis, obtaining the mechanical behaviour of these tubulars under service loads through experiment is an effective way to guarantee the safe and efficient of offshore drilling operations [3].

However, few literatures have reported the experimental equipment, which can impose external pressure to tubulars. There is a set of experimental system in the University of Rio De Janeiro, Brazil, which can provide 10 MPa water pressure, and the maximum simulated water depth is 1000 m, and the maximum operating depth of the fifth- and sixth-generation drilling platform (ship) is 3000 m. An experimental system named Mechanics Behaviour Simulation Experimental System for Deep Water Drilling and Production Strings has been developed to provide 30 MPa water pressure and to simulate external pressure of 3000 m water depth [4]. Until now, the system can impose external pressure, internal pressure, axial tension/compression load and lateral load to the tubulars, which provide a good platform for exploration and development of offshore oil and gas and can perfect deepwater drilling theory, reduce

http://dx.doi.org/10.5772/62315

corresponding operation risk and improve the safety and economy of deepwater oil and gas development.

2. Theory analysis of riser mechanical behaviour

Marine riser is the key equipment connecting subsea wellhead and floating drilling platform (ship) in deepwater drilling and exploration. The main functions of marine riser are to provide channel for drilling mud in the annulus of riser and drill pipe, support auxiliary lines, guide drilling tools and install the BOP. As riser mechanical behaviour has great impact on deepwater drilling engineering, we take the riser in service as example in this chapter. Then, the mechanical model and control equation have been established. Next, the model validation and sensitivity analysis have been presented. Finally, we get the key parameters to control its mechanical behaviour.

2.1. Mechanical model

The schematic diagram of deepwater drilling riser in service is shown in **Figure 1**.

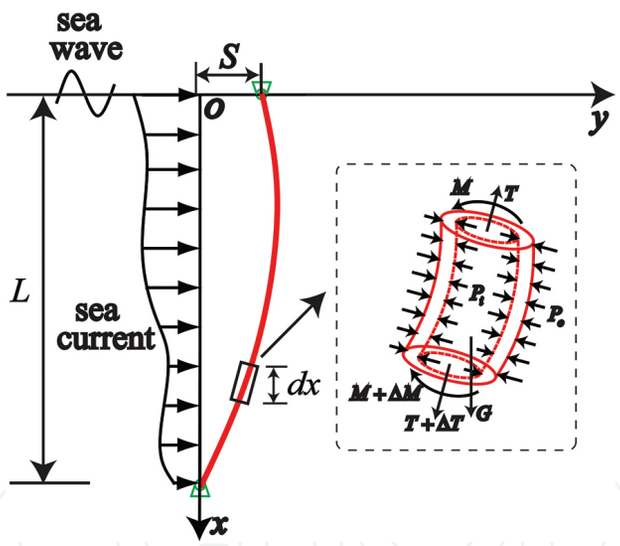

Figure 1. Static analysis model of riser mechanical behaviour.

The analysis model can be regarded as a beam located in the vertical plane and subjected to both non-uniform tension force and lateral force. Both the top and the end of riser are connected with the ball joints, so the boundary conditions are hinge constraints. Take the connection point of drilling ship and riser top as the origin of the coordinate, and the positive direction of x axis is vertical to the bottom of the sea, and the positive direction of y axis is the same as that of the lateral force. Besides, the following assumptions are applied during equation deduction:

- The material of riser is homogeneous, isotropic and linear elastic, and the riser bending stiffness is constant.

- The movement direction of sea wave and current is in the same plane.
- Top tension does not change with time.
- Riser curvature and torsion are small, and the geometric non-linearity is neglected.

The riser differential control equation can be represented as follows [5]:

$$\mathrm{EI}\frac{\mathrm{d}^4 y}{\mathrm{d}x^4} - T(x)\frac{\mathrm{d}^2 y}{\mathrm{d}x^2} - w\frac{\mathrm{d}y}{\mathrm{d}x} = F(x) \tag{1}$$

where EI(x) is the riser flexural rigidity along the x axis (N·m^2); $T(x)$ is the riser tension force distribution along the x axis (N); w is the per unit length weight of riser in sea water (N/m); $F(x)$ is the total lateral force distribution along the x axis (N).

As the top and end of the riser are connected with ball joints, the boundary conditions of Equation 1 can be written as follows:

$$\begin{cases} y\big|_{x=0} = S; \quad \theta\big|_{x=0} = 0 \\ y\big|_{x=L} = 0; \quad \theta\big|_{x=L} = 0 \end{cases} \tag{2}$$

2.2. Load calculations

2.2.1. Tension force

The main axial loads subjected on riser include gravity and top tension force, and the axial force of riser section at x below the sea surface can be represented by the following equation:

$$T(x) = T_{\mathrm{top}} - wx \tag{3}$$

where T_{top} is the top tension imposed on riser top end (N).

2.2.2. Lateral force

The main lateral force of riser is generated by sea wave and current. If ignoring the dynamic effects, the combined wave and current force can be calculated by the following equation:

$$F(x) = C_{\mathrm{D}}\rho D(v_{\mathrm{w}} + v_{\mathrm{c}})|v_{\mathrm{w}} + v_{\mathrm{c}}| / 2 + C_{\mathrm{m}}\rho\pi D^2 a_{\mathrm{w}} / 4 \tag{4}$$

where C_{D} is the drag force coefficient (a dimensionless quantity); C_{m} is the inertia force coefficient (a dimensionless quantity); ρ is the density of sea water (kg/m^3); D is the outer diameter of riser (m); v_{w} is the horizontal velocity of sea wave particle (m/s); v_{c} is the current velocity (m/s); $a_{\mathrm{w}} = \mathrm{d}wt/\mathrm{d}t$ is the horizontal acceleration of sea wave particle (m/s^2).

http://dx.doi.org/10.5772/62315

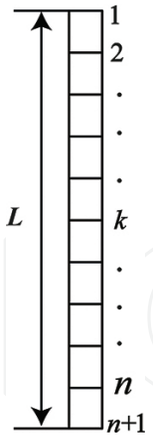

Figure 2. Riser discretisation model.

The sea current velocity under a certain depth of the sea surface can be calculated by the following equation recommend by American Bureau of Shipping:

$$v_c(x) = v_m(x/L)^{1/7} + v_t(x/L) \tag{5}$$

where v_m is the sea surface wind velocity (m/s); v_t is the sea surface tide velocity (m/s).

The linear wave theory is usually chosen to calculate the horizontal velocity of sea wave particle, and the equation is as follows:

$$v_w = \pi H / T_w \exp\left[k(x-L)\right]\cos(ky - \omega_w t) \tag{6}$$

where H is the wave height (m); T_w is the wave period (s); k is the wave number (a dimensionless quantity); ω_w is the wave circular frequency (rad/s).

Generally, the maximum of wave current is always used to calculate the maximum value of riser deformation and stress, and the maximum lateral force can be obtained through substituting Equations 5 and 6 into Equation 4.

2.3. Model solution

Equation 1 is very complex and cannot obtain the analytical solutions. In this chapter, we have solved Equation 1 by weighted residual method.

2.3.1. Residual equation

As shown in **Figure 2**, riser length can be divided into n spans. The first node locates at riser top and is marked with No. 1, the last node locates at riser end and is marked with No. (n + 1). So, the whole discrete elements have (n + 1) nodes and n elements.

Because Equation 1 is a fourth-order differential equation, the shape function in weighted residual method can be written as follows [6]:

$$y_i = C_{i,0} + C_{i,1}x + C_{i,2}x^2 + C_{i,3}x^3 + C_{i,4}x^4 + C_{i,5}x^5, \quad x \in [0, l_i], \ (i = 1, 2, \cdots, n+1) \tag{7}$$

where y_i is the displacement of discrete nodes; l_i is the length of each span; C_{ij} (j = 0, 1, 2, 3, 4, 5) is the undetermined coefficients.

The derivative forms of the shape functions are as follows:

$$\begin{cases} y_i' = C_{i,1} + 2C_{i,2}x + 3C_{i,3}x^2 + 4C_{i,4}x^3 + 5C_{i,5}x^4 \\ y_i'' = 2C_{i,2} + 6C_{i,3}x + 12C_{i,4}x^2 + 20C_{i,5}x^3 \\ y_i''' = 6C_{i,3} + 24C_{i,4}x + 60C_{i,5}x^2 \\ y_i^{(4)} = 24C_{i,4} + 120C_{i,5}x \end{cases}, \quad x \in [0, l_i], \ (i = 1, 2, \cdots, n+1) \tag{8}$$

Substituting Equations 7 and 8 into Equation 1, the residual equation can be written as follows:

$$R_i(x) = \mathrm{EI}_i y_i^{(4)}(x) - T_i(x) y_i''(x) - w_i y_i'(x) - F(x) \tag{9}$$

As the shape function determined by Equation 7 is fifth order, there are six undetermined coefficients C_{ij} (j = 0, 1, 2, 3, 4, 5) in each shape function. Besides, there are n discrete elements in the system, so there are 6n equations that are needed to solve the problem. Generally, two collocation points are needed in weighted residual method. If l_i/3 and 2l_i/3 are chosen as the collocation points, the residual value should be equal to 0 as follows:

$$\begin{aligned} &R_i\left(\frac{1}{3}l_i\right) = \mathrm{EI}_i\left(24C_{i,4} + 40C_{i,5}l_i\right) - T_i\left(\frac{1}{3}l_i\right)\left(2C_{i,2} + 2C_{i,3}l_i + \frac{4}{3}C_{i,4}l_i^2 + \frac{20}{27}C_{i,5}l_i^3\right) \\ &-w_i\left(C_{i,1} + \frac{2}{3}C_{i,2}l_i + \frac{1}{3}C_{i,3}l_i^2 + \frac{4}{27}C_{i,4}l_i^3 + \frac{5}{81}C_{i,5}l_i^4\right) - F_i\left(\frac{1}{3}l_i\right) = 0, \quad (i = 1, 2, \ldots, n) \end{aligned} \tag{10}$$

$$\begin{aligned} &R_i\left(\frac{2}{3}l_i\right) = \mathrm{EI}_i\left(24C_{i,4} + 80C_{i,5}l_i\right) - T_i\left(\frac{2}{3}l_i\right)\left(2C_{i,2} + 4C_{i,3}l_i + \frac{16}{3}C_{i,4}l_i^2 + \frac{160}{27}C_{i,5}l_i^3\right) \\ &-w_i\left(C_{i,1} + \frac{4}{3}C_{i,2}l_i + \frac{4}{3}C_{i,3}l_i^2 + \frac{32}{27}C_{i,4}l_i^3 + \frac{80}{81}C_{i,5}l_i^4\right) - F_i\left(\frac{2}{3}l_i\right) = 0, \quad (i = 1, 2, \ldots, n) \end{aligned} \tag{11}$$

2n equations can be obtained through Equations 10 and 11, other 4n equations are needed to list according to the boundary conditions and continuity conditions.

2.3.2. Continuity conditions

The continuity of geometry and physical properties of riser guarantees the continuity of displacement, deflection angle, bending moment and shear force on the adjacent discrete element as follows:

$$\begin{cases} x_i(l_i) = x_{i+1}(0) \\ \theta_i(l_i) = \theta_{i+1}(0) \\ M_i(l_i) = M_{i+1}(0) \\ Q_i(l_i) = Q_{i+1}(0) \end{cases}, (i = 2,3,\cdots,n) \tag{12}$$

According to the relationship among displacement, deflection angle, bending moment and shear force in mechanics of materials, the following equations can be listed after substituting Equations 7 and 8 into Equation 12 as follows:

$$\begin{cases} C_{i,0} + C_{i,1}l_i + C_{i,2}l_i^2 + C_{i,3}l_i^3 + C_{i,4}l_i^4 + C_{i,5}l_i^5 = C_{i+1,0} \\ C_{i,1} + 2C_{i,2}l_i + 3C_{i,3}l_i^2 + 4C_{i,4}l_i^3 + 5C_{i,5}l_i^4 = C_{i+1,1} \\ \mathrm{EI}_i\left(2C_{i,2} + 6C_{i,3}l_i + 12C_{i,4}l_i^2 + 20C_{i,5}l_i^3\right) = 2\mathrm{EI}_{i+1}C_{i+1,2} \\ \mathrm{EI}_i\left(6C_{i,3} + 24C_{i,4}l_i + 60C_{i,5}l_i^2\right) = 6\mathrm{EI}_{i+1}C_{i+1,3} \end{cases}, \quad (i = 2,3,\cdots,n) \tag{13}$$

4(n–1) equations can be obtained according to Equation 13, and 6n–4 equations can be listed through adding 2n equation as mentioned above. Other 4 equations can be acquired by boundary conditions.

2.3.3. Boundary conditions

The boundary conditions of the system are shown in Equation 2. Substituting the shape function and its derivative forms into Equation 2, the boundary conditions can be represented by the following equation:

$$\begin{cases} C_{1,0} = S; \quad C_{1,1} = 0 \\ C_{n+1,0} + C_{n+1,1}l_{n+1} + C_{n+1,2}l_{n+1}^2 + C_{n+1,3}l_{n+1}^3 + C_{n+1,4}l_{n+1}^4 + C_{n+1,5}l_{n+1}^5 = 0 \\ C_{n+1,1} + 2C_{n+1,2}l_{n+1} + 3C_{n+1,3}l_{n+1}^2 + 4C_{n+1,4}l_{n+1}^3 + 5C_{n+1,5}l_{n+1}^4 = 0 \end{cases} \tag{14}$$

4 equations can be obtained according to Equation 14, and all of the 6n equations have been obtained finally. In other words, the 6n undetermined coefficients and the displacement of the riser system can be determined unique. Once the deformation has been obtained, the internal force and strength can be discussed later.

2.4. Model validation

Taken a real deepwater drilling operation as example, the water depth is 1500 m, the riser outer diameter is 533.4 mm, the riser wall thickness is 15.875 mm, the top tension is 1.3 G, the top displacement of floating vessel is 30 m, the steel density is 7850 kg/m^3, the elastic modulus of steel is 206 GPa, the drilling fluid density is 1200 kg/m^3, the sea water density is 1030 kg/m^3, the wave height is 6.5 m, the wave period is 8 s, the sea surface wind velocity is 2 m/s, velocity of sea tide is 0.5 m/s, the drag force coefficient is 0.8 and the inertia force coefficient is 1.5.

Numerical simulations have been conducted with two-dimensional finite element model using ABAQUS software. The models are completed in the ABAQUS version 6.12-3 software. The computer used is DELL OPTIPLEX-390, and the RAM is 4 GB. Results of analysis calculated by the theoretical method and the numerical simulations are shown in **Figures 3** and **4**.

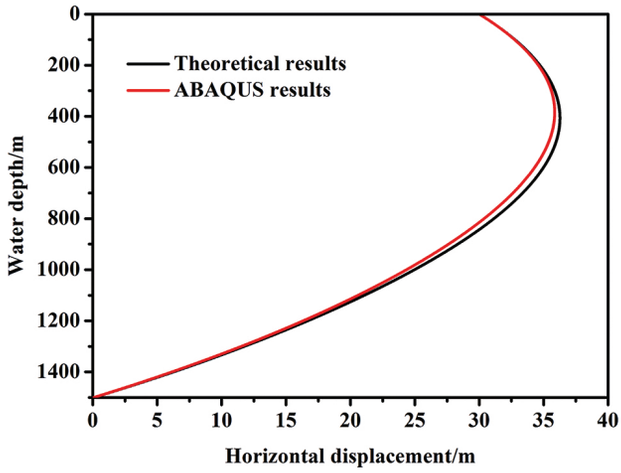

Figure 3. Horizontal displacement.

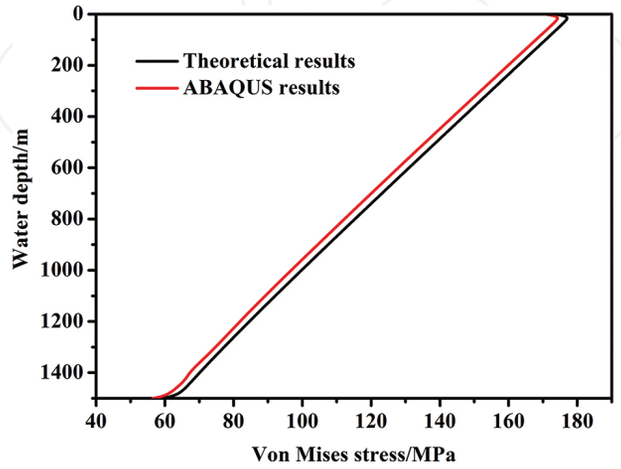

Figure 4. Von Mises stress.

http://dx.doi.org/10.5772/62315

As shown in **Figures 3** and **4**, good consistency has been shown between the calculation results, which validate the availability of the theoretical analysis. In particular, in regard to horizontal displacement, the maximum horizontal displacement calculated by theoretical analysis and ABAQUS software is 36.3 and 35.9 m, which locates at 406 and 383 m below the sea surface, and the maximum calculation error is 1.1% and 5.6%, respectively. However, in regard to stress, the Von Mises stress of the maximum value is 177 and 174 MPa, and both of them appear at 16 m below the sea surface.

3. Experimental system

3.1. System compositions

The experimental system is named mechanics behaviour simulation experimental system for deep water drilling and production strings, which has four sub-systems, namely mechanical structure, hydraulic power and control system and data acquisition system. The main system configuration is shown in **Figure 5** [7].

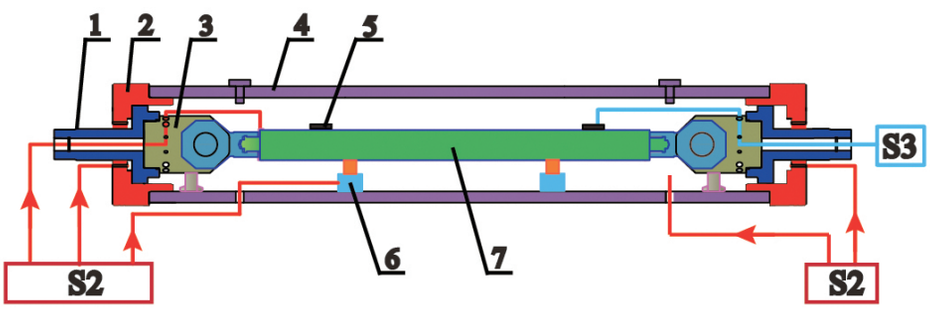

Figure 5. System compositions (1) axial piston; (2) end clamp; (3) connection joint; (4) main cylinder; (5) strain gauge; (6) hydraulic cylinder; (7) tubular specimen; (S2) hydraulic power and control system; (S3) data acquisition system.

The mechanical structure, which is the main body of the experimental equipment, is consist of the main cylinder, two axial pistons, two end clamps and two connection joints. The hydraulic power and control system includes proportion booster cylinder, servo booster cylinder and two hydraulic cylinders to apply transverse force. The main parameters of mechanical structure and hydraulic power and control system are shown in **Tables 1** and **2**.

Main cylinder				End clamp		
O.D. (mm)	I.D. (mm)	Length (mm)	P_w (MPa)	O.D. (mm)	I.D. (mm)	Stroke (mm)
1500	1200	8000	30	1000	400	220

Note: O.D. = outer diameter; I.D. = inner diameter; P_w = pressure-withstanding value.

Table 1. Main structure parameters of the experimental system.

	D_{ip} (mm)	D_p (mm)	Stroke (mm)	V_{max} (m/s)	γ	P_{max} (MPa)
C_1	180	120	700	0.5	2.25	56
C_2	180	120	700	1.0	1.65	46
C_3	140	80	100	–	–	25

Note: C_1, C_2, C_3 are proportion booster cylinder, servo booster cylinder and transverse hydraulic cylinders. D_{ip} = inner diameter of piston cylinder; D_p = outer diameter of piston rod; V_{max} = maximum output speed; γ = Booster ratio; P_{max} = maximum output pressure.

Table 2. Main parameters of the hydraulic control system.

Besides, the data acquisition system is consist of strain gauges and instruments for displacement, strain, pressure and flow rate measurement.

3.2. System working principle

3.2.1. Determination of simulated condition

Generally, we do small size simulation experiment, but in some cases, we need to conduct full size simulation experiment. So, the first matter is to decide which kind of the experiment is. Then, the experimental samples are needed to manufacture. However, no matter which kind of experiment is, we must know the loads subjected to the samples before the experiment. So, the simulated conditions are needed to clearly confirm. Next, the internal pressure, external pressure, axial force and lateral force subjected on the samples are in need for precise calculation . Finally, we must program the load spectrum and upload into the control system to be called during the experiment. It should be pointed out that, if the experiment is not a destructive test, we must limit the load to ensure the safety and integrity of the sample.

3.2.2. Sample installation and load applying

Once the load spectrum is accomplished, the tubular sample is needed to install into the main cylinder. The installation process should be based on the following procedures: first, the strain gauges should be pasted on the sample, and the test leads should connect to the data acquisition system, then connect the sample with one of the connection joint, the axial piston and the end clamp successively, then put the two lateral hydraulic cylinders into the main cylinder, then connect the hydraulic lines with the hydraulic system and then install the left axial piston and end clamp. When conducting the experiment, the hydraulic power system receives the instructions (pressure and displacement) from the control host, and apply internal pressure, external pressure, axial load and lateral force to the tubular sample. The tubular sample generates displacement and strain under the simulation loads. The displacement and strain signals transmit into the data acquisition system through the teat leads. And finally, the strain and stress state of the sample can be obtained by analysing the data.

3.2.3. Pressure relief

Pressure relief is necessary after the experiment. To ensure the safety of the specimen in pressure unloading, all kinds of loads are needed to be unloaded in proportion.

3.3. System main functions

3.3.1. External pressure-withstanding test

When the external pressure is generated by water pressure in the main cylinder, the axial piston will be pushed towards axially, which will result in axial tension at the tubular sample. In some cases, the axial tension may exceed the maximum allowable load and result in sample damage. So, when external pressure-withstanding tests are done in addition to the water pressure in the main cylinder, the pressure of water must be pumped into the annulus between the end clam and the axial piston to balance the axial force generated by water pressure in the main cylinder. Besides, these two kinds of water pressure must be pumped proportionally.

3.3.2. Internal pressure-withstanding test

Similarly, when the internal pressure is generated by water pressure in the tubular sample, the axial tension will also be appeared. So, when internal pressure-withstanding tests are done, the pressure of water in the sample and the annulus between the end clam and the axial piston must be pumped concurrently and proportionally.

3.3.3. Combination test under external, internal and lateral forces

If we want to study the mechanics performance of tubular under combined internal pressure, external pressure and lateral force, the pressure of water pumped in the main cylinder, tubular sample and the annulus between the end clam and the axial piston must be loaded concurrently and in proportion.

3.3.4. Sealing performance test

Many devices used in the deepwater engineering require good sealing performance. Since the experiment equipment can provide 30 MPa pressure, it is a good platform to conduct sealing performance test for some special devices.

3.4. System performance test

Through system debugging, the hydraulic power system has presented good performance in receiving and executing the instructions from the control host. Besides, the hydraulic servo valves have excellent performance in regulation of pressure and flow rate according to the feedback signals. No phenomenon of leaking water and oil has been occurred. All of the technical indicators have been reached in the laboratory. After completion of the debugging, the internal and external pressure loading tests have been completed, and the actual value collected by the data acquisition system and the target pressure value is shown in **Figure 6**.

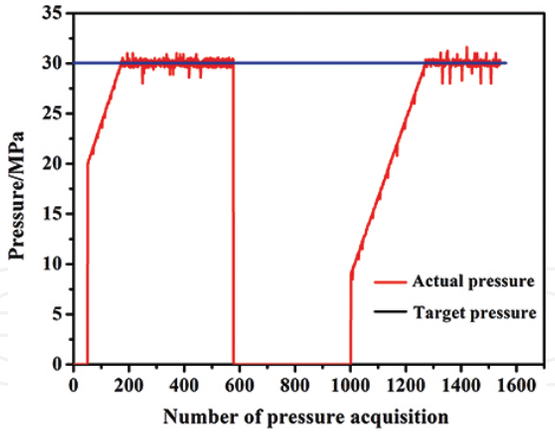

Figure 6. System performance test curve.

As shown in **Figure 6**, the pressure can rapidly response and remain unchanged for long time period. After pressure relief, the reload performance is still excellent. During pressure maintenance phase, the maximum pressure is 31.61 MPa, the minimum pressure is 28.15 MPa, and the average pressure is 29.97 MPa, which indicate that the pressure control system has outstanding performance and can carry out well in accordance with the experimental expectations.

4. Simulation experiments

4.1. Theoretical analysis

As shown in **Figure 1**, the marine drilling riser in working status is subjected to internal pressure, external pressure, axial tension and bending moment induced by drilling fluid, sea water, top tension and lateral force, respectively. If we choose micro-unit from riser outer wall surface, the stress state is shown in **Figure 7**.

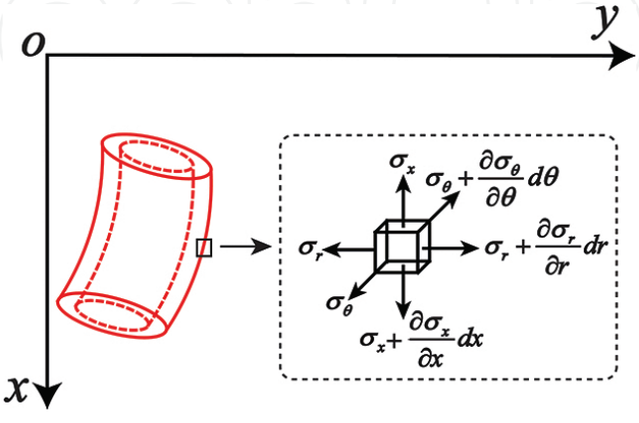

Figure 7. Stress state of riser outer wall surface.

http://dx.doi.org/10.5772/62315

As shown in **Figure 7**, the micro-unit is under the stress state of axial stress, radial stress and hoop stress, and all of the stresses are principal stress. The relationship between the stress and the loads is satisfied by the following equation:

$$\begin{cases} \sigma_{\mathrm{r}} = \dfrac{p_{\mathrm{i}}a^2 - p_{\mathrm{o}}b^2}{b^2 - a^2} - \dfrac{(p_{\mathrm{i}} - p_{\mathrm{o}})a^2b^2}{(b^2 - a^2)r^2} \\ \sigma_{\theta} = \dfrac{p_{\mathrm{i}}a^2 - p_{\mathrm{o}}b^2}{b^2 - a^2} + \dfrac{(p_{\mathrm{i}} - p_{\mathrm{o}})a^2b^2}{(b^2 - a^2)r^2} \\ \sigma_{\mathrm{x}} = \dfrac{F_{\mathrm{a}}}{S_{\mathrm{a}}} \pm \dfrac{M}{W} \end{cases} \tag{15}$$

where σ_θ is the hoop stress (Pa); σ_{r} is the radial stress (Pa); σ_{x} is the axial stress (Pa); a and b are the inner diameter and outer diameter of riser, respectively (m); p_{i} and p_{o} are the internal and external pressures, respectively (Pa); F_{a} is the axial tension (N); S_{a} is the cross-sectional area (m^2); M is the bending moment (N·m); W is the bending modulus (m^3); "+" is selected at the side under tension stress generated by bending moment, whereas "–" is applied at the side under compressive stress generated by bending moment.

Once the stress state has been obtained, the strain value of the micro-unit can be calculated by the generalized Hooke's law as follows:

$$\begin{cases} \varepsilon_r = \dfrac{1}{E}\left[\sigma_r - \mu\left(\sigma_\theta + \sigma_x\right)\right] \\ \varepsilon_\theta = \dfrac{1}{E}\left[\sigma_\theta - \mu\left(\sigma_r + \sigma_x\right)\right] \\ \varepsilon_x = \dfrac{1}{E}\left[\sigma_z - \mu\left(\sigma_\theta + \sigma_r\right)\right] \end{cases} \tag{16}$$

where ε_{r}, ε_θ and ε_{x} are the radial strain, hoop strain and axial strain, respectively, and E and μ are elastic modulus and Poisson's ratio, respectively.

As shown in **Figure 3**, the riser has the maximum horizontal displacement at about x = 400 m. Therefore, we select the riser here as the simulation object, and the theoretical calculation results of loads, stress and deformation are shown in **Table 3**.

P_{i} (MPa)	p_{o} (MPa)	F_{a} (N)	M (N·m)	σ_{x} (MPa)	σ_{r}/ (MPa)	σ_θ/ (MPa)	ε_{x} (με)	ε_{r} (με)	ε_θ (με)
4.8	4.0	3.08e6	1.78e4	124.8	−4	6.8	602	−211	−143

Table 3. Theoretical calculation results of riser at x = 400 m.

What calls for special attention is that ε_x and ε_θ can be obtained after experiment, while ε_r is difficult to be measured directly. However, if we use the theoretical value of radial stress, σ_x, ε_x and ε_θ are known in Equation 16, and σ_r, σ_θ and ε_r can be solved. So, finally, the stress state strength check can be determined by σ_x, σ_r and σ_θ.

4.2. Simulation experiment method

The four-point bending method has been adopted in the simulation experiment, and the mechanical analysis model of the tubular sample is shown in **Figure 8** [8].

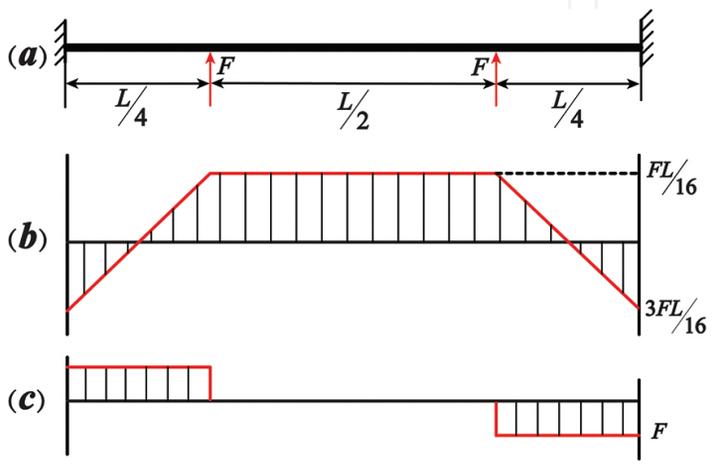

Figure 8. Simulation experiment method: (a) mechanical analysis model; (b) bending moment diagram of tubular sample and (c) shearing force diagram of tubular sample.

Because the two ends of the tubular sample are fixed with the connection joints, this constrain can be regarded as a fixed end. The force outputted by two lateral hydraulic cylinders pushes the sample upward. If both of the two outputted forces equal to F, then the bending moment between $L/2$ is constant and equals to $FL/16$. So, the tubular sample between $L/2$ is the real simulation object.

4.3. Key problems

4.3.1. Insulation problem between strain gauges and tubular sample

Because the strain gauges and its welding wires are working in high water pressure, the insulation between strain gauges and tubular sample must be done to avoid the high water pressure infiltrating into the strain gauge base. Otherwise, the strain gauge will separate from the sample, which will result in rapid drop of insulation resistance and even fall off of the strain gauges. All of these have strong impact on the accuracy of the measurement data. Besides, if the welding wires are exposed to high water pressure directly, the wires would be conductive with water, which will also result in distortion or even failure of the measurement. Therefore, the exposed metal parts in welding wires must be isolated from the water. Generally, the chemical coating method is used in strain measurement under high water pressure. Before the

experiment, the sealing protection measures must be adopted after the strain gauges are pasted on the outer wall of the tubular sample.

The measure taken to insulate the strain gauges is shown in **Figure 9**.

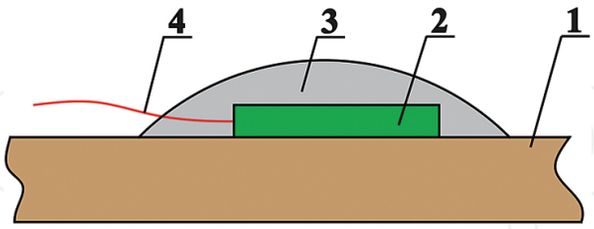

Figure 9. Sealing protection measures of strain gauges: (1) outer wall of the tubular sample; (2) strain gauge; (3) sealing glue and (4) test wires.

4.3.2. Sealing problems between test wires and the main cylinder

As the test leads connect the strain gauges and the strain acquisition instrument, which is put outside of the main cylinder, there must be satisfactory sealing problems between the test wires and the main cylinder. If the sealing measures do not conform to the requirements, the water leakage would happen during pumping water pressure, which would cause pressure fluctuations in the main cylinder and unstable strain signals. The key to solve this problem is to design reasonable sealing plugs. Design principles of the sealing plug are sealing easy and effective, large capacity of test leads, not complicated machinery manufacturing and installa-

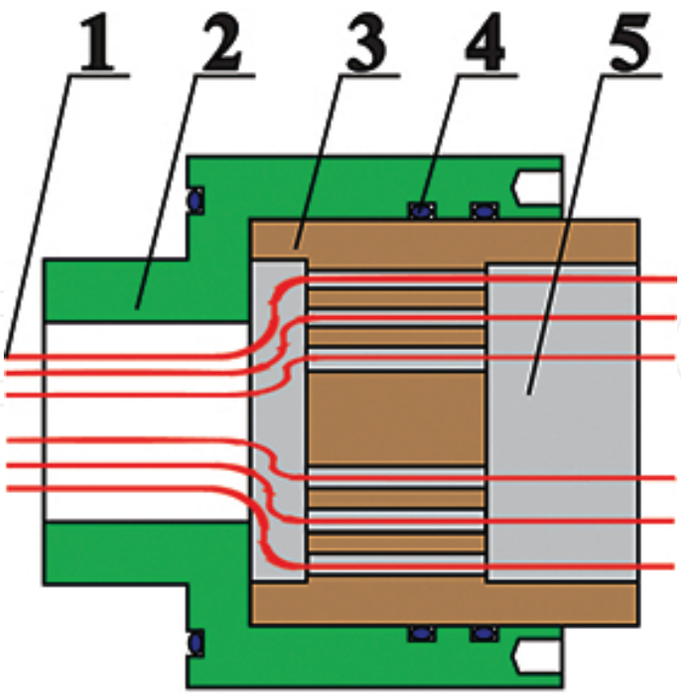

Figure 10. Sealing plug: (1) test wires; (2) sealing plug body; (3) sealing plug core; (4) seal rings and (5) sealing glue.

tion and the possibility to be reused. The comprehensive cleaning of residue and oil stain is necessary and important to ensure that the sealing performance of the plugs after manufacture is completed. In this experiment, sealing glue is used to inject into the plugs to seal them. Moreover, the sealing performance test must be conducted to ensure that the plugs meet the requirements of the pressure in the experiment. Otherwise, the sealing plugs need to be re-made. The sealing measure taken to seal the test wires and the main cylinder is shown in **Figure 10**.

4.4. Tubular sample

The tubular sample is a steel pipe, with a length of 6000 m, outer diameter of 520 mm, inner diameter of 496 mm (wall thickness is 12 mm) and Elastic modulus and Poisson's ratio of 206 GPa and 0.3, respectively.

4.5. Pressure loading scheme

According to **Table 3**, the bending moment subjected to the sample is 1.78e4 N·m, so the force outputted by the lateral hydraulic cylinders is 18.5 MPa based on the experiment equipment shown in **Table 2**. So, there are three parameters needed to be controlled, which are the internal pressure (4.8 MPa), the external pressure (4.0 MPa) and the lateral hydraulic pressure (18.5 MPa). Equal proportion loading scheme has been selected in the experiment, as shown in **Figure 11**.

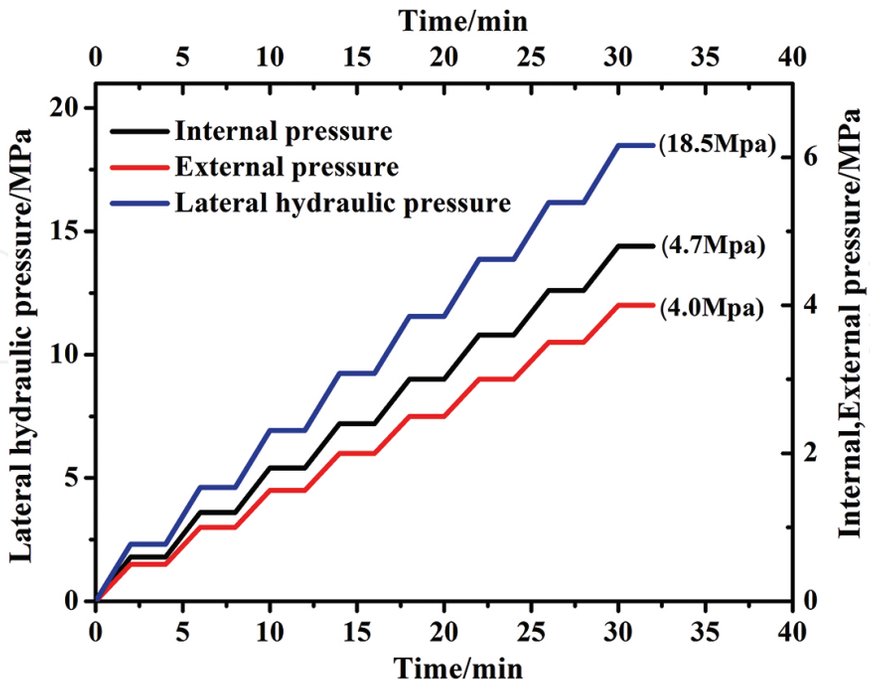

Figure 11. Pressure loading scheme.

http://dx.doi.org/10.5772/62315

As shown in **Figure 11**, the loading scheme of "pressurization–stabilization–pressurization–stabilization…" is adopted. The displacement, pressure and flow rate are collected at all the experimental time, while the strain of the sample is only collected during pressure stabilization period. In each load period, the pressurization duration is 2 min, and the stabilization duration is 2 min. So, the duration of each load period is 4 min. After each load period, the increases of internal pressure, external pressure and lateral hydraulic pressure are about 0.6, 0.5 and 2.31 MPa, and the three kinds of pressure will eventually achieve 4.7, 4.0 and 18.5 MPa, respectively, after 8 load periods. Then, the stress state of the tubular sample reaches that of the marine riser at x = 400 m. To acquire more valid data, the duration of stabilization can be extended as expected after 32 min.

4.6. Strain gauges pasted scheme

As shown in **Figure 8**, four-point bending method is used in the experiment, and the tubular sample between $L/2$ is the real simulation object. So, the strain gauges are all pasted on this section. The whole scheme of pasting strain gauges is shown in **Figure 12**.

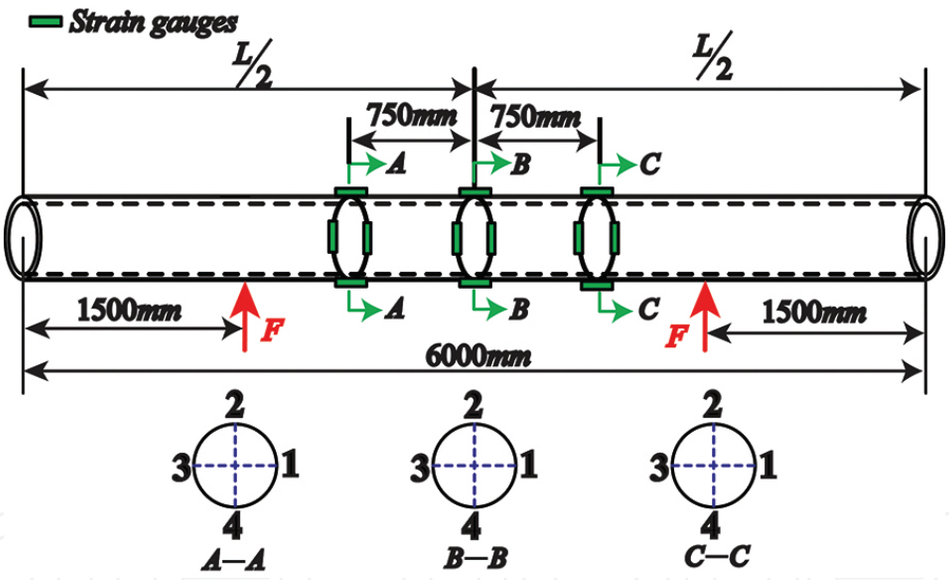

Figure 12. Strain gauges pasted scheme of the whole sample.

To acquire more valid data on different section, three sections (A–A, B–B and C–C) have been chosen to paste the strain gauges. One section locates the centre of the sample, and the other two sections symmetrically locate 750 mm from the centre of the sample. On each section, there are four points (1, 2, 3, 4), and the circumference interval of the four points is 90°, as shown in **Figure 12**. To measure the axial strain and hoop strain simultaneously, there are two strain gauges that are pasted at each point, of which one pasting direction is coincidence with the one of the mother lines of the tubular sample, and the other pasting direction is perpendicular to the prior strain gauge. The pasting scheme at each point is shown in **Figure 13**.

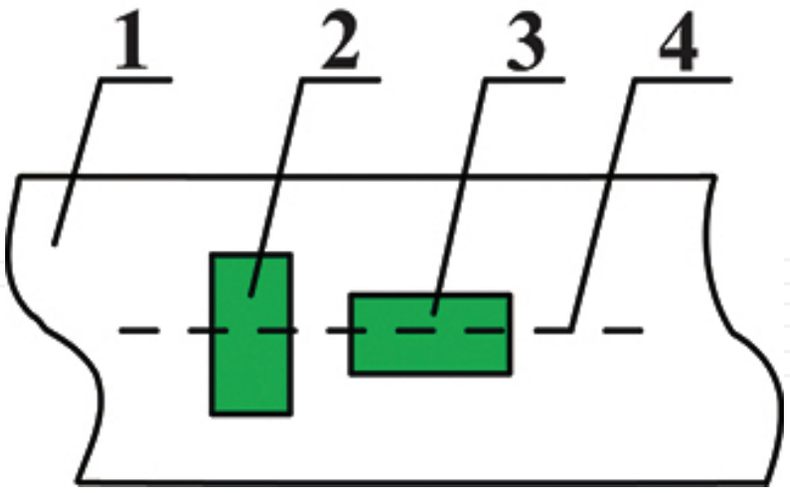

Figure 13. Pasting scheme at each point.

Therefore, 8 strain gauges are pasted at each section, and 24 strain gauges are pasted at the whole sample, of which 12 strain gauges measure the axial strain, and other 12 strain gauges measure the hoop strain. From theoretical perspective, the hoop strains measured at each point are equal, whereas the axial strains measured at point are unequal (Point 2 > Point 1 = Point 3 > Point 4).

4.7. Pressure acquisition

According to the experiment purpose, the three kinds of pressure (internal pressure, external pressure and lateral hydraulic pressure) are measured real time. The actual measured value of the pressure during stabilization period is shown in **Figure 14**.

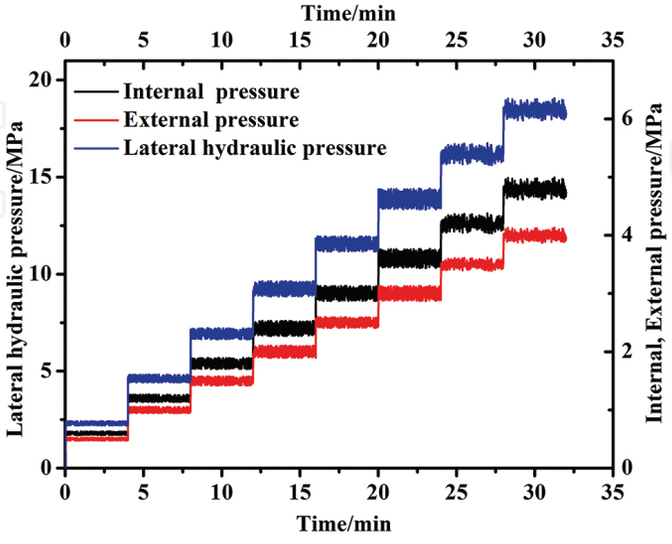

Figure 14. Measured pressure value.

http://dx.doi.org/10.5772/62315

As shown in **Figure 14**, good feedback adjustment has been revealed. Although the actual value has fluctuated during pressure loading, they generally increase in the forms of steps. Finally, all of the pressure values have reached the experiment expectation with high consistency, and the average values of the internal pressure, external pressure and lateral hydraulic pressure are 4.8, 4.1 and 18.5 MPa, respectively. Besides, during the stabilization duration, the strain data have been measured successfully.

4.8. Strain acquisition

The average strain values of the tubular sample under 4.8, 4.1 and 18.5 MPa are shown in **Table 4**.

Measure points	Strain value		Measure points	Strain value		Measure points	Strain value	
	ε_x (με)	ε_θ/ (με)		ε_x (με)	ε_θ/ (με)		ε_x/ (με)	ε_θ/ (με)
A-1	609	−147	B-1	603	−144	C-1	598	−150
A-2	639	−149	B-2	633	−133	C-2	622	−150
A-3	608	−134	B-3	606	−137	C-3	601	−134
A-4	587	−149	B-4	578	142	C-4	570	−151

Table 4. Strain data measured by the gauges.

As shown in **Table 4**, all of the strain gauges have collected the strain data during the experiment, which indicates that the key problems (insulation problem between strain gauges and tubular sample and sealing problems between the test wires and the main cylinder) involved in the experiment have been solved effectively, and the strain of the tubular sample can be measured by the experiment method as mentioned above.

4.9. Data analysis

Due to the influence of the bending moment, the axial strain at the same section is different. The average value of the axial strain at Points 1, 2, 3 and 4 are 604, 631, 605 and 578 με, respectively, which verifies the above analysis (Point 2 > Point 1 = Point 3 > Point 4). However, if we take the axial strain (29 με) induced by the bending moment (1.78 × 104 N·m) into consideration, the axial point of the four points can be represented by the following: Point 2 = Point 1 + 29 με = Point 3 + 29 με and Point 1 = Point 3 = Point 4 + 29με. The hoop strain is approximately equal at the 12 measure points, and both of the theoretical value and the average value of the measured value are –143 and –143 με, which verifies the accuracy of the experiment method. The theoretical and measured axial strains are shown in **Figure 15**.

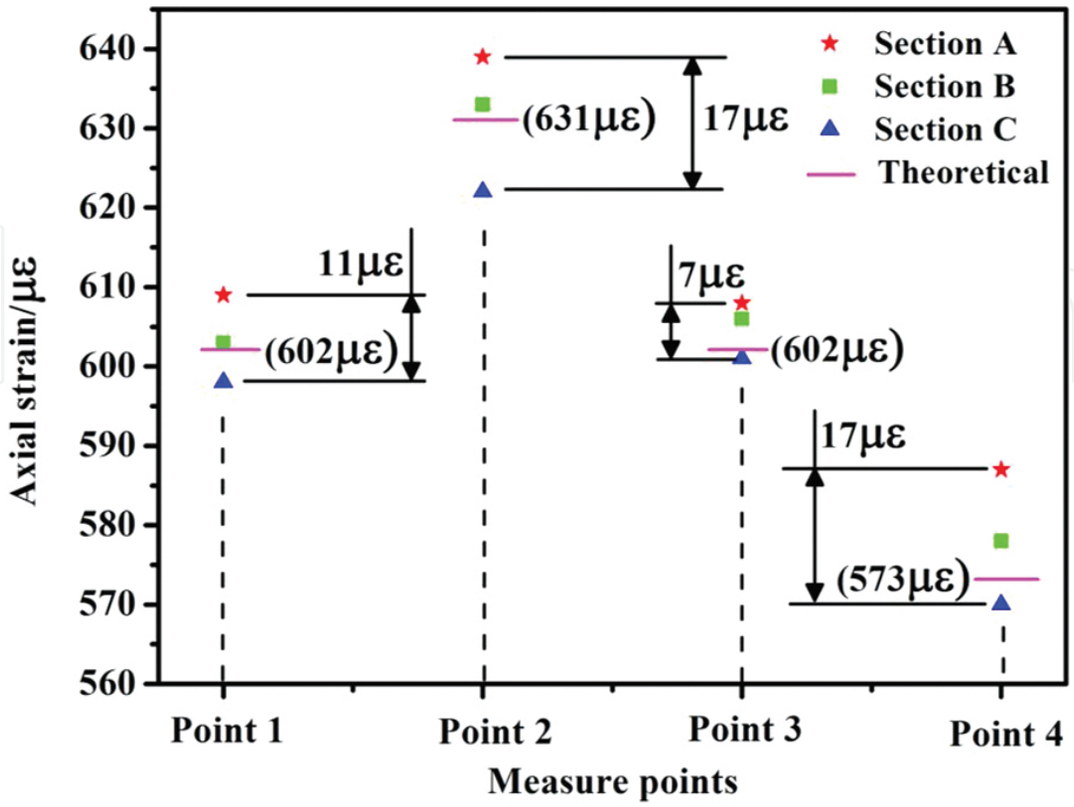

Figure 15. Theoretical and measured value of axial strains.

As shown in **Figure 15**, the maximum differences of the four measure points at the three sections are 11, 17, 7 and 17 με. If we take the average of the three sections at the same point, the statistical results can be as presented in **Table 5**.

Items	Point 1	Point 2	Point 3	Point 4
Theoretical value (με)	602	631	602	573
Average of the measured value (με)	603	631	605	578
Error (%)	0.2	0	0.5	0.9
Variance ($με^2$)	22	50	18	86

Table 5. Statistical results of the measure axial strain.

4.10. Stress state analysis

Because the radial strain cannot be measured directly, the stress state can be determined by the theoretical axial stress, the measured hoop strain and axial strain according to Equation 16. After analysis, the stress state of the experimental sample under the eight stabilization phases is shown in **Figure 16**.

http://dx.doi.org/10.5772/62315

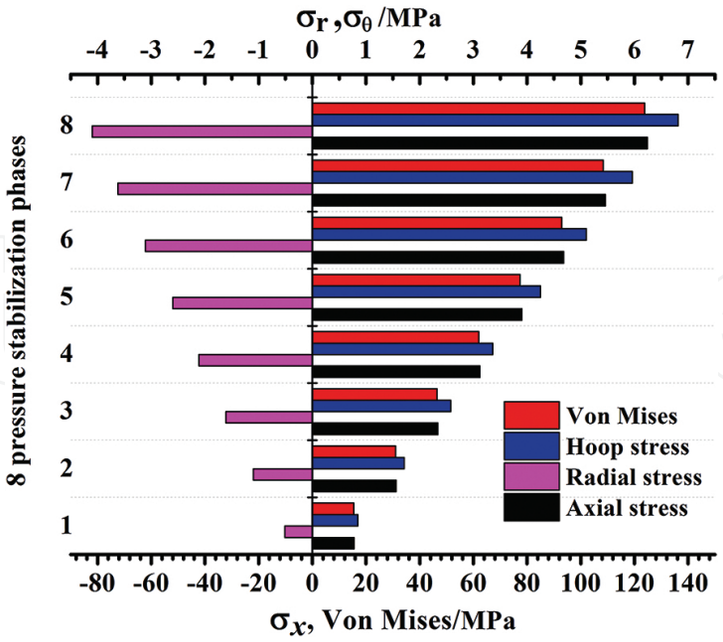

Figure 16. Stress state analysis.

As shown in **Figure 16**, with the increases of internal pressure, external pressure, axial tension and bending moment, the hoop stress, radial stress, axial stress and the Von Mises stress increase gradually. When the loads' state reaches the simulation condition required in the experiment, the Von Mises stress is 121.9 MPa, while the theoretical value is 123.8 MPa. The measurement error is only 1.5%, which verifies the feasibility and validity of the simulation experiment method.

5. Conclusion

Internal pressure, external pressure, axial tension and bending moment are typically loads subjecting on the tubulars in offshore drilling engineering. The mechanical model and control equations have been established to analyse the deformation and stress distribution of the marine riser, and the analysis method has been verified by finite element method (FEM) in the ABAQUS framework.

The experimental system has the ability to provide kinds of loads to simulate the mechanical behaviour of offshore tubulars, which exhibits a good platform to studying the mechanics of tubulars under complicated stress state and can perfect the deepwater drilling from theoretical viewpoint and field practice.

Good solutions must be proposed to solve the key problems in the simulation experiment, and thus, the technique of strain test under high water pressure can be used to measure the strain data effectively. Besides, excellent pressure loading scheme and the strain acquisition scheme are necessary to acquire precise measurement results.

Acknowledgements

The authors gratefully acknowledge the financial support from the Natural Science Foundation of China (NSFC, 51521063, U1262201)

Author details

Yanbin Wang*, Deli Gao and Jun Fang

*Address all correspondence to: wyb576219861@126.com

MOE Key Laboratory of Petroleum Engineering, China University of Petroleum, Beijing, China

References

[1] Gao Deli. (2011).Optimized Design and Control Techniques for Drilling & Completion of Complex-Structure Wells. China University of Petroleum Press, Beijing, China, ISBN 978-7-5636-3598-6.

[2] Lu Baoping. (2014). Key Technologies and Equipment for Deepwater Drilling. China Petrochemical Press, Beijing, China, ISBN 978-7-5114-2695-6.

[3] Robello Samuel & Gao Deli. (2013). Horizontal Drilling Engineering: Theory, Methods and Applications. Sigma Quadrant Publisher, Texas, USA, ISBN: 978-0-615-83770-3.

[4] Wang Yanbin, Gao Deli & Fang Jun. (2014). Development of Mechanics Behavior Simulation Experimental System for Deep Water Drilling and Production String. Oil Field Equipment, Vol. 43, No. 4, pp: 26–29.

[5] Wang Yanbin, Gao Deli & Fang Jun. (2014). Static analysis of deep-water marine riser subjected to both axial and lateral forces in its installation. Journal of Natural Gas Science and Engineering, Vol. 19, pp: 84–90.

[6] Gao Deli & Zhang Hui. (2012). Mechanical Analysis of Tubes in Deepwater Drilling Operation without Riser. Science & Technology Review, Vol. 30, No. 4, pp: 37–42.

[7] Fang Jun, Wang Yanbin & Gao Deli. (2013). Test Method for the Force Deformation of Deepwater Riser. China Petroleum Machinery, Vol. 41, No. 12, pp: 53–57.

[8] Liu Hongwen. (2011). Mechanics of Materials. Higher Education Press, Beijing, China, ISBN: 978-7-0403-0895-2.